High-resolution magnetic resonance spectroscopy in unstable fields *via* intermolecular zero-quantum coherences

Meijin Lin,[ab] Xi Chen,[a] Shuhui Cai[a] and Zhong Chen*[ab]

Received 29th September 2009, Accepted 1st March 2010
First published as an Advance Article on the web 28th April 2010
DOI: 10.1039/b920180g

Intermolecular zero-quantum coherences (iZQCs) have been utilized to achieve high-resolution nuclear magnetic resonance (NMR) proton spectra under inhomogeneous and/or unstable fields. In this paper, we demonstrated that despite the insensitivity of iZQCs to B_0 variations, the influence of unstable fields on the observable single-quantum coherence signals causes strong t_1 noises in the high-resolution iZQC spectra. Short-time acquisition (STA) and phase spectrum schemes were proposed for noise suppression in *in vivo* iZQC magnetic resonance spectroscopy (MRS) under temporal B_0 variations. The feasibility of these schemes were verified by localized spectroscopic studies under B_0 variations generated by the Z0 coil current oscillations and by voxel position variations in the presence of field gradients, which simulate the field conditions of MRS in the presence of physiological motions. The phase scheme not only improves the signal-to-noise ratio but also further reduces the linewidth by half.

1. Introduction

There are many circumstances that nuclear magnetic resonance (NMR) studies are subject to inhomogeneous and unstable magnetic fields, such as *in vivo* magnetic resonance microscopy (MRM), and ultra-high field NMR using externally powered magnets. High-field *in vivo* proton magnetic resonance spectroscopy (MRS) is not only subject to inhomogeneous line broadening caused by susceptibility gradients, but also often greatly degraded by field instability during averaging. The drifts of the main magnetic fields, which are between 0.05–0.1 ppm h^{-1} at 4 T systems and above, are one source of unstable fields.[1] Other than the main magnet, gradient coil vibrations caused by Lorentz forces also superimpose period modulations on the B_0 and thus induce sideband artifacts in MRS studies.[2,3] Furthermore, physiological motions in inhomogeneous fields cause precession frequency varying from time to time in thoracic, abdominal and even brain MRS.[4] Another source of time-dependent B_0 variations is respiratory-induced bulk susceptibility change in the chest, which can extend far from the chest.[5] Concerning the effects of physiological motion in brain and breast, the displacement is small relative to the voxel size. Rather than voxel misregistration, small-scale motions produce phase and frequency variations during experiments.[6] In breast MRS, for instance, motion-induced B_0 variations are mainly caused by respiration: the B_0 variation period is $\sim$4 s and the frequency shift was reported to be $\sim$0.14 ppm at various static field strengths.[6,7] The phase variations induced by B_0 fluctuations lead to signal cancellation in data summation, while the frequency variations result in line broadening. Several techniques, either retrospective[6,8] or prospective,[9,10] were proposed to compensate the destructive summation in the presence of B_0 variations. However, these techniques, focusing on unstable-field effects, can hardly suppress the line broadening caused by inhomogeneous fields. On the other hand, high-resolution methods under inhomogeneous fields, such as the Fourier synthesis based algorithms[11,12] and nutation echoes,[13] are not designed for high-resolution spectroscopy under temporal B_0 variations or *in vivo* susceptibility gradients. The spatial encoding single-shot 2D spectroscopy technique[14] was also utilized to achieve high-resolution 1D and 2D spectroscopy[15,16] and MR imaging[17,18] under severe magnetic field distortions. In a very recent work,[19] Pelupessy and co-workers used coherence transfers between spins such as the SECSY sequence instead of spatially-dependent *z*-rotations[15,16] to compensate inhomogeneities with a modified single-shot 2D spectroscopy using the adiabatic sweep for encoding.[20,21] Theoretically, coherence/polarization transfers between spins can compensate arbitrary field inhomogeneities with larger spatial scales than the distance between coupled spins,[22] so that the new method is also promising in *in vivo* applications with randomly distributed magnetic field gradients.

As another kind of spin coherence transfer, intermolecular multiple-quantum coherences (iMQCs) come from distant dipolar couplings between spins.[23,24] It is reported that intermolecular zero-quantum coherence (iZQC) sequences, such as HOMOGENIZED[24] and its derivations,[25–27] and intermolecular double-quantum coherence (iDQC) sequences named IDEAL[28] and IDEAL-II[29] are capable of improving spectral resolution in inhomogeneous fields with magnetic susceptibilities varying over distances much larger than the correlation distance between coupled spins. The *in vivo* iZQC MRS has been performed on biological samples and rodents,[30–32] and the feasibility of this technique has been

[a] *Department of Physics, Fujian Key Laboratory of Plasma and Magnetic Resonance, State Key Laboratory of Physical Chemistry of Solid Surface, Xiamen University, Xiamen 361005, China. E-mail: chenz@xmu.edu.cn; Fax: +86 (0)592 2189426; Tel: +86 (0)592 2181712*
[b] *Key Laboratory of Under water Acoustic Communication and Marine Information Technology, Ministry of Education, Xiamen University, Xiamen 361005, China*

studied numerically[33] and reviewed.[34] Lin and co-workers proposed the CPMG-HOMOGENIZED sequence, which combines HOMOGENIZED with Carr–Purcell–Meiboom–Gill (CPMG), and performed a novel study with this sequence on a 25 T electromagnet, achieving the first high-resolution liquid NMR spectrum at a field >1 GHz.[35] Since the insensitivity of iZQC to inhomogeneous/unstable fields has been demonstrated previously,[24,35] the current work will focus on the phase deviations that unstable fields impose on the iZQC signals and their influences on the spectrum. Theoretical analysis shows that the evolutions of non-zero coherence orders, *e.g.* the directly detected single-quantum coherences (SQCs), are susceptible to random phase deviations under unstable fields. The CPMG scheme eliminates the phase deviations during the echo time, but does not correct those during the other t_2 acquisition time. These phase deviations will lead to strong phase noise in 2D iZQC spectra and cause a great reduction of the signal-to-noise ratio (SNR) of the desired high-resolution projection spectrum onto the F1 dimension. To suppress the phase deviations during the t_2 period, the t_2 frequency evolution subject to the influence of unstable fields should be eliminated and the frequency information such as chemical shifts should be discarded in the F2 dimension. Two schemes, short-time acquisition (STA) and phase spectrum schemes are proposed herein to achieve this goal for MRS subject to B_0 variations. Localized spectroscopic studies were performed on the agar gel phantom to test these schemes under simulated magnetic field conditions for MRS with physiological motion.

2. Theory

Consider a homogeneous solution consisting of two isolated homonuclear spin-1/2 systems, denoted as I and S respectively. It is assumed that ω_m is the frequency offset of spin m ($m = I, S$) in the rotating frame in the absence of magnetic field inhomogeneity, and $\Delta B(\mathbf{r})$ is the deviation from the static field B_0 at position $\mathbf{r}$. When spatially dependent magnetic field is taken into account, the frequency offset, $\Omega_m(\mathbf{r})$, of spin m at position $\mathbf{r}$ is given by

$$\Omega_m(\mathbf{r},t) = \omega_m + \Delta\omega(\mathbf{r},t) = \omega_m + \gamma\cdot\Delta B(\mathbf{r},t),\ (m = I, S) \quad (1)$$

where γ is the gyromagnetic ratio.

The HOMOGENIZED pulse sequence is depicted in Fig. 1a. The desired coherence transfer pathway (CTP) is $0 \rightarrow 0 \rightarrow +1 \rightarrow -1$. The effects of radiation damping, diffusion and transverse relaxation are ignored in the following deduction.

One of the mirrored pathways desired, $I_zS_z \rightarrow I^-S^+$ $(t_1) \rightarrow I_zS^+ \rightarrow I_zS^-$, is explored to demonstrate the effects of an unstable and inhomogeneous field. During the t_1 period, the term in this pathway evolves as

$$\tfrac{1}{4}I^-S^+ \exp\{i[-\omega_I - \Delta\omega(\mathbf{r},t) + \omega_S + \Delta\omega(\mathbf{r},t)]t_1\} = \tfrac{1}{4}I^-S^+ \exp[i(-\omega_I+\omega_S)t_1]. \quad (2)$$

Since the correlation distance, within the range of which are the distances between the most distantly dipolar-coupled spins, is of a magnitude order of 10–100 μm (60 μm in the current work), relatively much smaller than the macroscopic spatial variations of the static magnetic field. So $\Delta\omega_I(\mathbf{r}) \approx \Delta\omega_S(\mathbf{r})$, and eqn (2) is approximately valid.

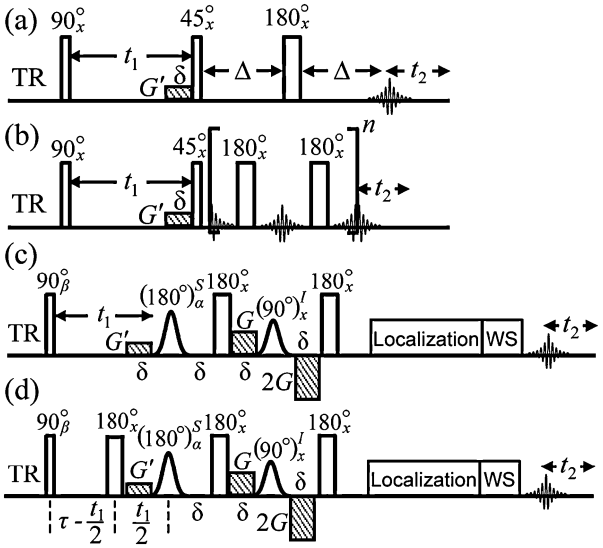

Fig. 1 Pulse sequences: (a) HOMOGENIZED, (b) CPMG-HOMOGENIZED, (c) modified iDH, and (d) homo-decoupled modified iDH. Gauss-shapes indicate soft pulses selective for spin S or I only. TR is the repetition time between scans. "Location" and "WS" blocks are spatial localization module and water suppression module using excitation sculpting scheme, respectively.

After the second RF pulse, eqn (2) is converted into

$$-\frac{i}{4}\sin\frac{\pi}{4}\cos^2\frac{\pi}{8}I_zS^+ \exp[i(-\omega_I+\omega_S)t_1]. \quad (3)$$

During the first Δ period, eqn (3) evolves as

$$-\frac{i}{4}\sin\frac{\pi}{4}\cos^2\frac{\pi}{8}I_zS^+ \exp[i(-\omega_I+\omega_S)t_1] \cdot\exp\left[i\omega_S\Delta + i\int_0^{\Delta}\Delta\omega(\mathbf{r},t)\,\mathrm{d}t\right]. \quad (4)$$

After the third RF pulse and during the second Δ period, eqn (4) evolves under the unstable and inhomogeneous field as

$$-\frac{i}{4}\sin\frac{\pi}{4}\cos^2\frac{\pi}{8}I_zS^- \exp[i(-\omega_I+\omega_S)t_1] \cdot\exp\left[i\omega_S\Delta + i\int_0^{\Delta}\Delta\omega(\mathbf{r},t)\,\mathrm{d}t\right]\cdot\exp\left[-i\omega_S\Delta - i\int_{\Delta}^{2\Delta}\Delta\omega(\mathbf{r},t)\,\mathrm{d}t\right]$$

$$=-\frac{i}{4}\sin\frac{\pi}{4}\cos^2\frac{\pi}{8}I_zS^- \exp[i(-\omega_I+\omega_S)t_1] \cdot\exp\left[i\int_0^{\Delta}\Delta\omega(\mathbf{r},t)\,\mathrm{d}t - i\int_{\Delta}^{2\Delta}\Delta\omega(\mathbf{r},t)\,\mathrm{d}t\right]. \quad (5)$$

During the t_2 period, the signal is

$$-\frac{i}{4}\sin\frac{\pi}{4}\cos^2\frac{\pi}{8}S^{-}\exp[i(-\omega_I+\omega_S)t_1]$$
$$\cdot\exp\left[i\int_0^{\Delta}\Delta\omega(\mathbf{r},t)\,\mathrm{d}\tau - i\int_{\Delta}^{2\Delta}\Delta\omega(\mathbf{r},t)\,\mathrm{d}\tau\right] \quad (6)$$
$$\cdot\exp\left\{i\left[\omega_S t_2+\int_0^{t_2}\Delta\omega(\mathbf{r},t)\,\mathrm{d}\tau\right]\right\}.$$

where t denotes all the time slices during the scanning time, including t_1 and t_2. It can be seen from eqn (2)–(6) that in the t_1 period, the frequency perturbation factors due to unstable and inhomogeneous fields are canceled for the desired iZQC terms $I^{-}S^{+}$ (or its mirrored iZQC term $I^{+}S^{-}$), while the useful chemical shift information is preserved. Unlike iZQCs, SQCs of the detection period (t_2) are sensitive to inhomogeneous line broadening and unstable perturbation. In an inhomogeneous but stable field, the line broadening of SQCs in the F2 dimension does not hinder the high-resolution projection of iZQCs in the F1 dimension. However, the perturbation of unstable field not only leads to frequency variation of SQCs in the F2 dimension, but also produces random phases varying with t_1. Under unstable fields, the t in the term $\Delta\omega(\mathbf{r},t)$ in eqn (6) not only includes t_2 but also t_1, because the magnetic field strength varies from scan to scan. As a result, the t_1-dependent phase variation caused by $\Delta\omega(\mathbf{r},t)$ is Fourier transformed into t_1 noises in the frequency domain. Lin and co-workers proposed the CPMG-HOMOGENIZED sequence shown in Fig. 1b to eliminate the perturbation of phase accumulation during the spin–echo period (2Δ) through the CPMG scheme. In Fig. 1b, 2Δ is divided into $2n$ segments with each interval of $2\Delta/2n$. If the magnetic field variation period (T_m) is much larger than $2\Delta/2n$, the phase accumulation in each pair of segments with a π pulse in their middle can be cancelled:

$$\exp\left[i\int_{k\Delta/2n}^{(k+1)\Delta/2n}\Delta\omega(\mathbf{r},t)\,\mathrm{d}\tau - i\int_{(k+1)\Delta/2n}^{(k+2)\Delta/2n}\Delta\omega(\mathbf{r},t)\,\mathrm{d}\tau\right]$$
$$\xrightarrow{T_m\gg 2\Delta/2n}\exp[i\Delta\omega(\mathbf{r},t)\cdot(\Delta/2n)-i\Delta\omega(\mathbf{r},t)\cdot(\Delta/2n)]=1, \quad (7)$$

where k is an even number and $0 \le k \le 2n-2$. Therefore, the influence of unstable and inhomogeneous fields can be canceled in the total spin-echo period (2Δ). However, the frequency variation during t_2 $\left(\int_0^{t_2}\Delta\omega(\mathbf{r},t)\,\mathrm{d}\tau\right)$ still leads to random phase perturbation for each t_1 increment and thus produces t_1 noise.

From eqn (6), it can be seen that the frequency perturbation in the t_2 period can hardly be removed except by setting $t_2 = 0$, *i.e.* the signal is only acquired at the echo maximum. Spectral information such as chemical shift in the F2 dimension will also be removed in this way. However, the iZQC high-resolution spectroscopy obtains the spectral information from the F1 dimension instead of F2, so the chemical shift in F2 can be discarded. In the following section, two schemes, STA and phase spectrum, are proposed to utilize this theory to improve SNR.

The HOMOGENIZED sequence is also modified (Fig. 1c) to facilitate the *in vivo* applications. The intermolecular double-quantum filter (iDQF)[27] has been proposed to suppress the water conventional SQC signal as well as undesired resonances. The sequence in the current work is based on the iDQF-HOMOGENIZED sequence[27] (abbreviated as iDH). Since selective pulses are utilized, their performance in unstable fields should be examined. It has been demonstrated that the typical field situations of respiration-sensitive MRS are with the variation periods of $\sim$4 s and the frequency shifts of $<$0.4 ppm.[1,6] A Gaussian pulse with a duration of $\sim$4 ms (with a bandwidth $\sim$500 Hz) can be utilized for water suppression without exciting the nearest metabolite resonance at an 11.7 T system. Its pulse length is much shorter than the B_0 variation periods, so the performance of the selective excitation is hardly disturbed. Furthermore, the bandwidth of the selective pulse can adequately cover the frequency shift range of B_0 variations. Unlike iZQCs, iDQCs are sensitive to the unstable field. Therefore, a refocusing π pulse is placed in the middle of the iDQF, which is also much shorter than the B_0 variation period. Since B_0 modulation in MRS study is much slower than in NMR using externally powered magnet,[35] the Carr–Purcell train during the spin echo is replaced by a single π pulse for better water suppression. The spatial localization and the following excitation sculpting module utilized for water suppression (marked as the "Localization" and "WS" modules respectively in the pulse sequence schematics in Fig. 1) are also applied.

3. Experimental

All experiments were performed at 298 K using a Varian NMR System 500 MHz spectrometer with a 5 mm indirect detection probe with pulsed field gradient (PFG) modules. To simulate the situation of the MRS studies in the presence of motions and B_0 variations, we performed a series of spatially localized studies with the position of the voxel shifted from scan to scan and the current in the Z0 coil varied from time to time. The sample was an agar gel phantom containing 90 mM creatine (Cr) and 30 mM lactate (Lac). The voxel size was $3 \times 3 \times 12$ mm^3, where 12 mm was the localization length in the z direction. The voxel position was randomly shifted between -2.4 mm to 2.4 mm along the z direction. The Z0 current was modulated to produce B_0 fluctuations with a variation range of 60 Hz and a period of 4 s. This field condition was set according to ref. 1 and 6 to simulate the moderate *in vivo* field fluctuations caused by respiratory motion. The conventional MRS was acquired using the point-resolved spectroscopy (PRESS) sequence with the variable power and optimized relaxation delays (VAPOR) module for water suppression. The scan number was 32. For all iDH spectra, 400 points were acquired with a spectral width of 2500 Hz in the F1 dimension. The fold-over of the F1 dimension can be corrected since there is no resonance in the left-half of the F1 dimension. The spectral width of the direct dimension was 5000 Hz and the sampling time was 200 ms for the modified iDH. A 4-step phase cycling was applied: α = (x, y, x, y), β = (x, x, $-x$, $-x$) and the receiver = (x, x, x, x). The parameters (strength $\times$ duration) of coherence

selective gradients (CSGs) were $G' = 0.07$ T m^{-1} $\times$ 1.2 ms, $G = 0.16$ T m^{-1} $\times$ 1.2 ms, $G_1 = 0.14$ T m^{-1} $\times$ 1.0 ms, and $G_2 = 0.24$ T m^{-1} $\times$ 1.0 ms, respectively, where G_1 and G_2 are the spoiling PFGs in the WS module. The SNR was measured by dividing the peak height of Cr (3.0 ppm) resonance by the root-mean-square noise level between 2.0 and 2.4 ppm. The Cr (3.0 ppm) resonance was also used for the linewidth measurements. An exponential function with a line broadening factor of 3 Hz was applied in the indirect dimension of the iDH spectra with homo-decoupling.

4. Results and discussion

To simulate the situation of MRS study in the presence of motions, we performed a series of spatially localized studies with the position of the voxel shifted from scan to scan. Firstly, a PRESS spectrum was acquired in a well-shimmed magnetic field. No frequency variation can be observed from scan to scan (Fig. 2a). The z-direction shimming coils were then deliberately detuned to produce a moderate inhomogeneous line broadening of 50 Hz.[36] It can be seen that the resonance frequencies vary from scan to scan due to the background magnetic field gradients (Fig. 2b). It has been demonstrated that the change of bulk susceptibility in the chest also creates time-dependent B_0 variations.[5] Therefore, the current in the Z0 coil was modulated to produce B_0 variations within a range of 0.12 ppm and a period of 4 s to simulate the unstable fields caused by bulk susceptibility changes.[1,6] The PRESS spectrum from each scan is presented in Fig. 2c. The frequency variations mainly lead to line broadening in conventional 1D MRS. As demonstrated above, they cause severe t_1 artifacts in 2D spectra. A series of iZQC studies were performed under the same voxel position shifts and Z0 variations. Fig. 3a is the spectrum from the modified iDH sequence. Strong t_1 noises are observed in the 2D spectrum and the SNR of the projection spectrum was greatly reduced. To suppress the t_1 noises, a rectangular post-processing function of 1.5 ms width was applied, only preserving a few data points around the echo maximum. Such a scheme is dubbed short time acquisition (STA). Since the B_0 variation amplitude $\Delta\omega(\mathbf{r},t)$ in MRS is much smaller than the one in NMR under unstable fields, extending t_2 from 0 to circa 1 ms can preserve parts of chemical shift in the F2 dimension without leading to much increased contamination of the t_1 noises. As a result, the residual water t_1 ridge can be separated from the desired metabolite peaks in the F2 dimension, so it can be partly cut off when projecting onto the F1 axis and its influence on the SNR of the projection spectrum can be greatly reduced. The spectrum from the modified iDH sequence with the STA scheme is presented in Fig. 3b. The same experimental data as Fig. 3a was used with a 1.5 ms-width rectangular post-processing function applied on the echo maximum in the time domain. Since the acquisition time is very short, the broadened peaks stretch along the F2 dimension. However, it can be seen from the 2D spectrum and its projection onto the indirect dimension that the t_1 noises are greatly reduced. The projection spectra with different acquisition window width are presented in Fig. 4. It shows that the SNR grows as the acquisition time decreases.

The projection cross-section theorem states that the projection of a 2D phase-sensitive spectrum onto the indirect dimension forms an FT pair with the time-domain signals at $t_2 = 0$.[37] Therefore, it seems that theoretically an F1 projection of the iDH spectrum in phase display mode cannot only provide a phase-sensitive spectrum with improved linewidth, but also eliminate the t_1 noises due to unstable fields if the t_2 acquisition begins at the echo maximum! The experimental result (Fig. 3c, the same data as Fig. 3a in phase display mode) verifies this deduction: although severe t_1 noises remain in the 2D spectrum, they cancel each other and result in a noise-free

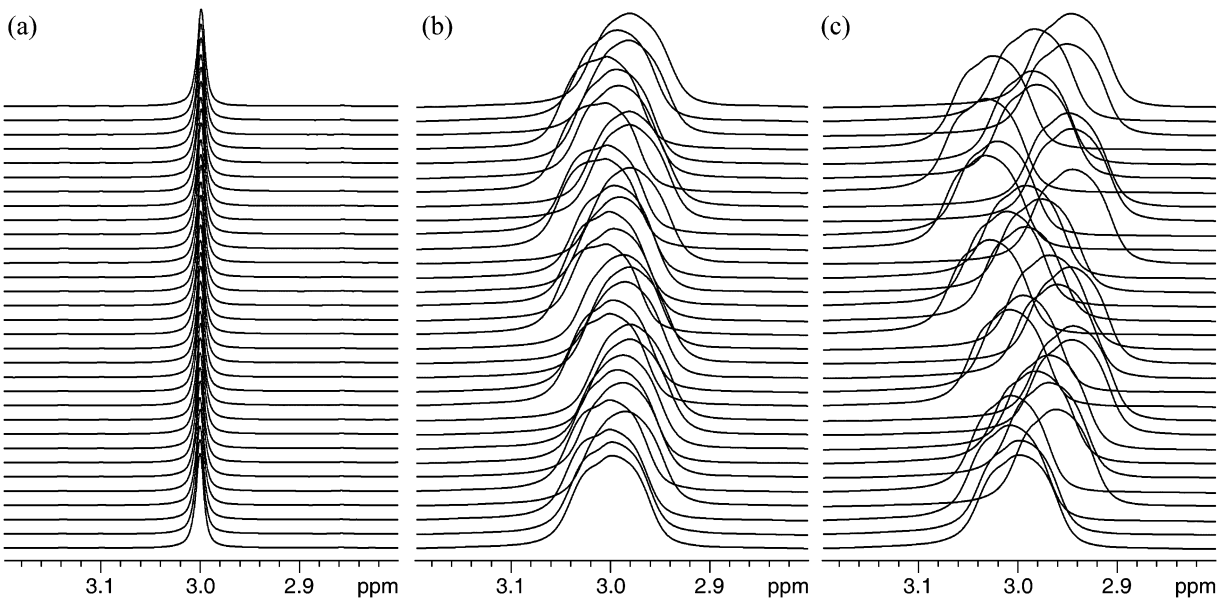

Fig. 2 PRESS spectra of an agar gel phantom containing 90 mM Cr and 30 mM Lac with the position of the voxel shifted from scan to scan: (a) in a well-shimmed magnetic field; (b) in an inhomogeneous field with a linewidth of 50 Hz; (c) in an unstable field with B_0 variations within a range of 60 Hz and a frequency of 0.25 Hz. The Cr (3.0 ppm) resonance was presented.

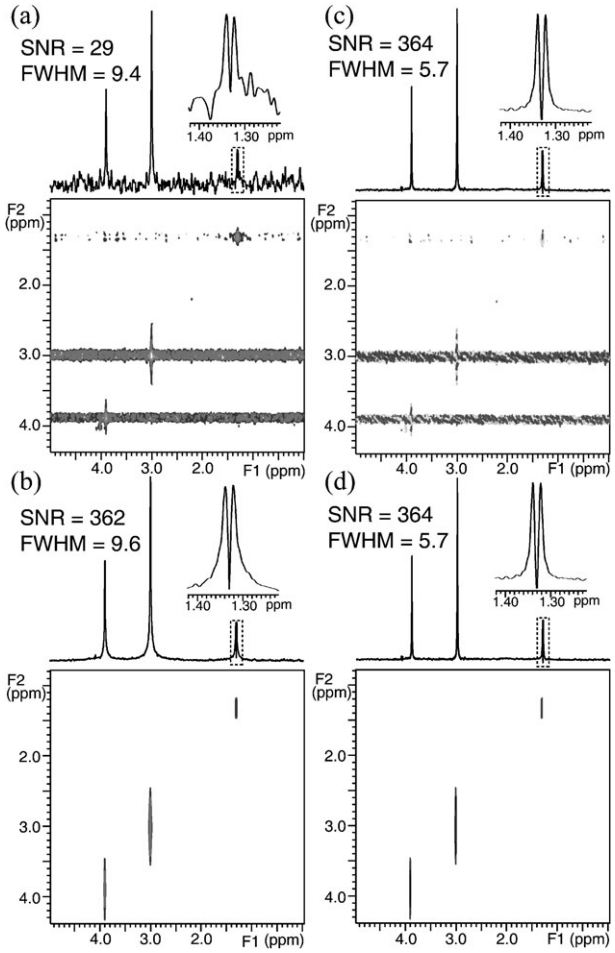

Fig. 3 Spectra from iDH sequence with a single refocusing π pulse: absolute-value spectra (a) without and (b) with STA, and phase-mode spectra (c) without and (d) with STA. All the spectra are from the same experimental data.

projection. Instead of direct accumulation of 2D data points, the projections of all the phase-sensitive spectra in the current work were calculated by the Fourier transformation of an interferogram compiled from the single complex point at echo maximum per value of t_1 increment because the manufacturers' software generally introduces systematic distortions that improve the appearance of spectra but distort the results of 2D projection. For comparison, the 2D phase-sensitive iDH spectrum with the STA scheme is also presented (Fig. 3d). Despite the different 2D spectral pattern, the projection and the measured SNR are exactly the same as those in Fig. 3c, which further confirms the theory. On the other hand, it should be noted that Fig. 3c and d have different intrinsic SNR (the ratio of the required signal to the background of thermal noise), though they have same signal-to-t_1-noise ratio (the ratio of the required signal to the pseudorandom noise that results from the effect of instabilities during the t_1 encoding). The intrinsic SNRs of Fig. 3c and d are 342 and 725, respectively. They are calculated on the 1D spectra of the direct dimension, using the same measurement as for the SNRs of the projection spectra. The higher intrinsic SNR of Fig. 3d is due to the reason that more effective data points were acquired and averaged.

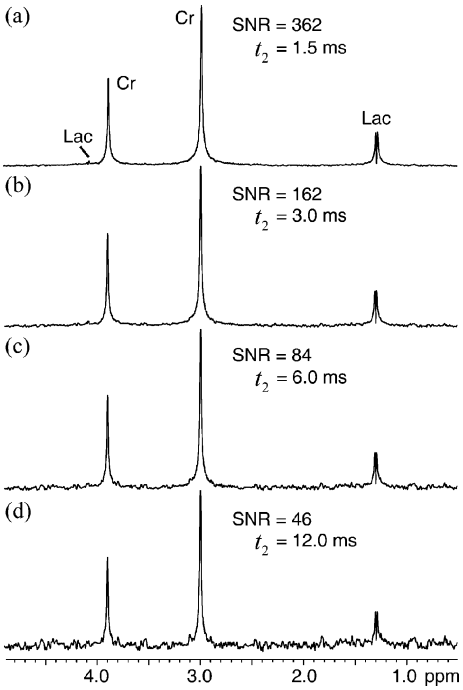

Fig. 4 Projection spectra from iDH sequence with STA and different acquisition time (t_2).

The projection spectra with different acquisition start time, which is defined as the deviation from the echo maximum, are presented in Fig. 5. It shows that the SNR reduces as the time deviation from the echo maximum increases.

If the constant-time scheme[38] is utilized in the iZQC period (Fig. 1d), a high-resolution homo-decoupled proton spectrum

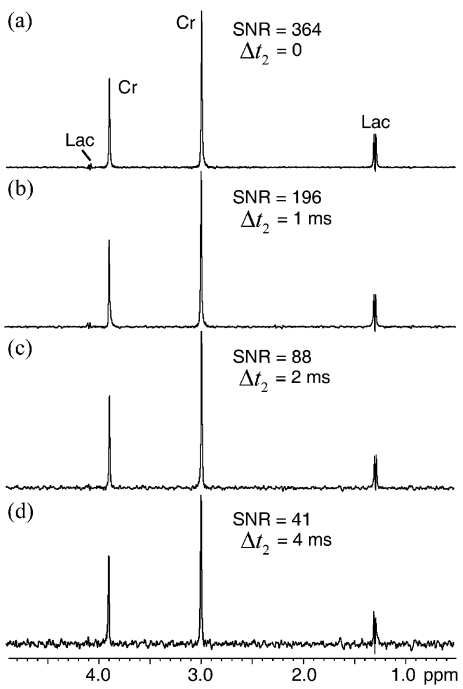

Fig. 5 Projection spectra from iDH sequence in phase display mode with different acquisition beginning time deviating from the echo maximum (Δt_2).

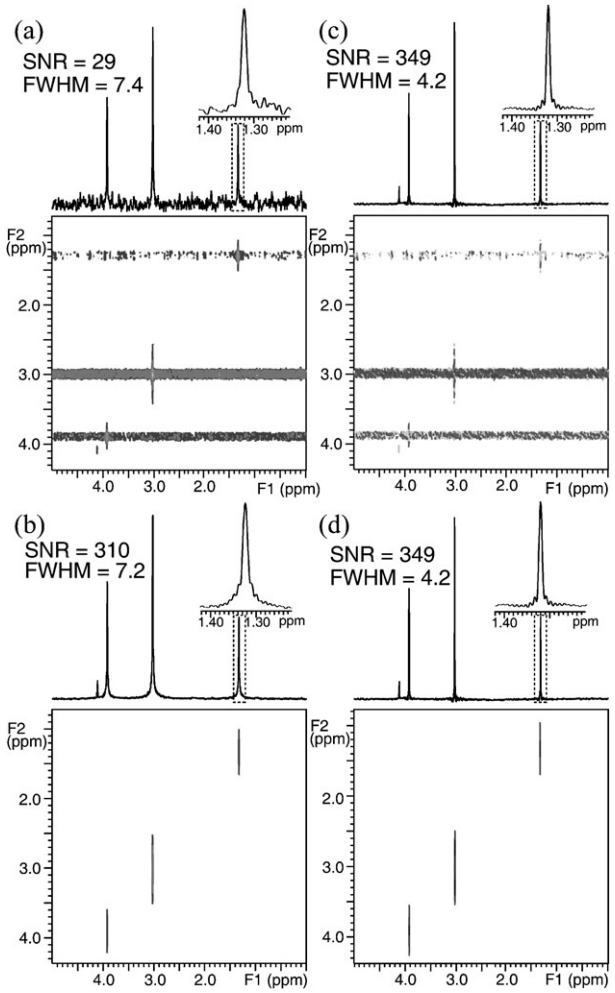

Fig. 6 Homo-decoupling spectra: absolute-value spectra (a) without and (b) with STA, and phase-mode spectra (c) without and (d) with STA. All the spectra are from the same experimental data.

can be achieved in inhomogeneous and unstable fields. Homo-decoupling experiments were performed under the same condition as Fig. 3 and the results are presented in Fig. 6. The absolute-value spectra without and with STA, and phase-mode spectra without and with STA are displayed in Fig. 6a–d, respectively. All the spectra in Fig. 6 are from the same experimental data. The linewidth and the SNR of each projection spectrum are given. It should be noted that the amplitudes of the *J*-coupled spins in the homo-decoupled spectrum are subject to *J* modulations, which is inherent for the constant-time module and can be alleviated by averaging the results from different constant-time lengths.[38]

In unstable B_0 field, the phase variations may originate from B_0 drifts before refocusing; in the presence of motion, the phase variations may be due to sample position shifts between coherence selection gradient (CSG) pairs. In our experiments, the variation period was rather long (4 s) compared to the pulse sequence time scale (several milliseconds), so the phase variations were hardly observable. It is the same for iZQC spectra. Otherwise, in the case of fast B_0 modulation/physiological motion, such as in MRS studies of the heart and abdomen, the phase variation effects of the iDH sequence should be carefully analyzed. The influence of motions between CSG pairs in iMQC sequences is somehow different from conventional MRS: the signal in the detection period is not only refocused by CSGs but also demodulated by the DDF. It takes some time for the DDF to go into effect. The length of this delay, usually called "demagnetizing time", is *circa* 100 ms at 11.7 T. It has been demonstrated[39,40] that the motion during the rather long demagnetizing time in the iMQC sequence hardly causes artifacts, since the DDF is generated by the sample itself and it moves at the same place as the sample.

Concerning the timescale of the instabilities, there are certain high-pass filters designed to suppress the effects of instabilities on a timescale longer than that over which experimental data are measured in real time. For functional MRI studies, they are used to filter out low-frequency baseline drift between activation periods.[47] For example, a high-pass filter of $(120\ \mathrm{s})^{-1}$ was used in ref. 47. In our study, the timescales of the proposed methods are much shorter, designed to suppress physiological-motion-induced instabilities (*e.g.* respirations with a period of circa 4 s). For the STA method the timescale is 1.5 ms, which is its effective acquisition period; for the "phase spectrum" method it is of the order of 400 μs, which is the inverse of the real-time filter bandwidth (spectral width in F2 is ±2500 Hz). It can be seen that the "phase spectrum" method has higher filtering threshold than the STA one, which means that it is less sensitive to high-frequency fluctuations. However the penalty is the lower intrinsic SNR, because the shorter the data acquisition period, the broader the bandwidth of thermal noise that contributes to the measured signal.

There are still some critical problems for *in vivo* applications of the new method proposed here. The scanning time (*circa* 1 h) of iZQC spectroscopy is almost unbearable for *in vivo* studies. Fast acquisition schemes such as fold-over correction,[41] star-pattern gradients scheme[42] and spatial encoded 2D spectroscopy[14,21] are promising to improve the scanning efficiency of iDH sequence under unstable fields. The weak iMQC signal intensity compared to SQCs is another critical problem for *in vivo* applications. Novel magnetization modulation scheme[43] and dynamic nuclear polarization[44,45] may be potentially useful for iMQC signal intensity enhancement. The multiple-echo read-out scheme for iMQC MRI may also be adopted in spectroscopy for signal to noise ratio optimization or 2D detection efficiency improvement.[46]

5. Conclusions

In this paper, the origin of t_1 noises in the iZQC high-resolution spectra under unstable fields was theoretically analyzed. A modified iDH sequence and two schemes of STA and phase spectrum were proposed for MRS to suppress the effects of physiological motions or B_0 variations *in vivo* as well as inhomogeneous broadenings. One of these schemes, the phase spectrum scheme, cannot only improve the SNR of the projection spectrum but also further reduce its linewidth by half. The primary results on phantoms under field fluctuations caused by Z0 current oscillations and voxel position-shifts verify the theoretical analysis of the proposed schemes. Further improvements of the new method for *in vivo* studies are underway.

Acknowledgements

This work was partially supported by the NNSF of China under Grants 10774125, 10875101 and 10974164, and the Research Fund for the Doctoral Program of Higher Education of China under Grant 200803840019.

References

1 T. Thiel, M. Czisch, G. K. Elbel and F. Hennig, *Magn. Reson. Med.*, 2002, **47**, 1077.
2 P. J. Bolan, L. DelaBarre, E. H. Baker, H. Merkle, L. I. Everson, D. Yee and M. Garwood, *Magn. Reson. Med.*, 2002, **48**, 215.
3 T. W. Nixon, S. McIntyre, D. L. Rothman and R. A. de Graaf, *J. Magn. Reson.*, 2008, **192**, 209.
4 R. Katz-Brull and R. E. Lenkinski, *Magn. Reson. Med.*, 2004, **51**, 184.
5 D. Raj, A. W. Anderson and J. C. Gore, *Phys. Med. Biol.*, 2001, **46**, 3331.
6 P. J. Bolan, P. G. Henry, E. H. Baker, S. Meisamy and M. Garwood, *Magn. Reson. Med.*, 2004, **52**, 1239.
7 I. S. Haddadin, A. McIntosh, S. Meisamy, C. Corum, A. L. S. Snyder, N. J. Powell, M. T. Nelson, D. Yee, M. Garwood and P. J. Bolan, *NMR Biomed.*, 2009, **22**, 65.
8 J. M. Tyszka and J. M. Silverman, *Magn. Reson. Med.*, 1998, **39**, 1.
9 M. V. McConnell, V. C. Khasgiwala, B. J. Savord, M. H. Chen, M. L. Chuang, R. R. Edelman and W. J. Manning, *Magn. Reson. Med.*, 1997, **37**, 148.
10 P. M. Pattany, I. H. Khamis, B. C. Bowen, K. Goodkin, R. G. Weaver, J. B. Murdoch, M. J. D. Post and R. M. Quencer, *Am. J. Neuroradiol.*, 2002, **23**, 225.
11 B. Pryor and N. Khaneja, *J. Chem. Phys.*, 2006, **125**, 194111.
12 H. Arthanari, D. Frueh, G. Wagner, B. Pryor and N. Khaneja, *J. Chem. Phys.*, 2008, **128**, 214503.
13 C. A. Meriles, D. Sakellariou, H. Heise, A. J. Moule and A. Pines, *Science*, 2001, **293**, 82.
14 L. Frydman, T. Scherf and A. Lupulescu, *Proc. Natl. Acad. Sci. U. S. A.*, 2002, **99**, 15858.
15 B. Shapira and L. Frydman, *J. Am. Chem. Soc.*, 2004, **126**, 7184.
16 B. Shapira and L. Frydman, *J. Magn. Reson.*, 2006, **182**, 12.
17 A. Tal and L. Frydman, *J. Magn. Reson.*, 2006, **182**, 179.
18 R. Paquin, P. Pelupessy and G. Bodenhausen, *J. Magn. Reson.*, 2009, **201**, 199.
19 P. Pelupessy, E. Rennella and G. Bodenhausen, *Science*, 2009, **324**, 1693.
20 P. Pelupessy, *J. Am. Chem. Soc.*, 2003, **125**, 12345.
21 P. Pelupessy, L. Duma and G. Bodenhausen, *J. Magn. Reson.*, 2008, **194**, 169.
22 Z. Chen, M. J. Lin, X. Chen and S. H. Cai, *Sci. China, Ser. G: Phys. Mech. Astron.*, 2009, **52**, 58.
23 W. S. Warren, W. Richter, A. H. Andreotti and B. T. Farmer, *Science*, 1993, **262**, 2005.
24 S. Vathyam, S. Lee and W. S. Warren, *Science*, 1996, **272**, 92.
25 D. Balla and C. Faber, *Chem. Phys. Lett.*, 2004, **393**, 464.
26 Z. Chen, T. Hou, Z. W. Chen, D. W. Hwang and L. P. Hwang, *Chem. Phys. Lett.*, 2004, **386**, 200.
27 X. Chen, M. J. Lin, Z. Chen, S. H. Cai and J. H. Zhong, *Phys. Chem. Chem. Phys.*, 2007, **9**, 6231.
28 Z. Chen, Z. W. Chen and J. H. Zhong, *J. Am. Chem. Soc.*, 2004, **126**, 446.
29 Z. Chen, S. H. Cai, Z. W. Chen and J. H. Zhong, *J. Chem. Phys.*, 2009, **130**, 084504.
30 C. Faber, E. Pracht and A. Haase, *J. Magn. Reson.*, 2003, **161**, 265.
31 D. Z. Balla, G. Melkus and C. Faber, *Magn. Reson. Med.*, 2006, **56**, 745.
32 D. Z. Balla and C. Faber, *Mag. Reson. Mater. Phys. Biol. Med.*, 2007, **20**, 183.
33 D. Z. Balla and C. Faber, *J. Chem. Phys.*, 2008, **128**, 154522.
34 D. Z. Balla and C. Faber, *Concepts Magn. Reson.*, 2008, **32a**, 117.
35 Y. Y. Lin, S. Ahn, N. Murali, W. Brey, C. R. Bowers and W. S. Warren, *Phys. Rev. Lett.*, 2000, **85**, 3732.
36 P. G. Henry, P. F. van de Moortele, E. Giacomini, A. Nauerth and G. Bloch, *Magn. Reson. Med.*, 1999, **42**, 636.
37 R. R. Ernst, G. Bodenhausen and A. Wokaun, *Principles of Nuclear Magnetic Resonance in One and Two Dimensions*, Clarendon Press, Oxford, 1987.
38 A. Bax, A. F. Mehlkopf and J. Smidt, *J. Magn. Reson.*, 1979, **35**, 167.
39 S. D. Kennedy and J. H. Zhong, *Magn. Reson. Med.*, 2004, **52**, 1.
40 T. Lin, H. J. Sun, Z. Chen, R. Y. You and J. H. Zhong, *Magn. Reson. Imaging*, 2007, **25**, 1409.
41 X. Chen, M. J. Lin, Z. Chen and J. H. Zhong, *Magn. Reson. Med.*, 2009, **61**, 775.
42 G. Galiana, R. T. Branca and W. S. Warren, *J. Am. Chem. Soc.*, 2005, **127**, 17574.
43 R. T. Branca, G. Galiana and W. S. Warren, *J. Chem. Phys.*, 2008, **129**, 054502.
44 E. R. Jenista, R. T. Branca and W. S. Warren, *J. Magn. Reson.*, 2009, **196**, 74.
45 M. Mishkovsky, U. Eliav, G. Navon and L. Frydman, *J. Magn. Reson.*, 2009, **200**, 142.
46 J. T. Schneider and C. Faber, *Magn. Reson. Med.*, 2008, **60**, 850.
47 R. Turner, A. Howseman, G. E. Rees, O. Josephs and K. Friston, *Exp. Brain Res.*, 1998, **123**, 5.

